



New modified carrier-based level-shifted PWM control for NPC rectifiers considered for implementation in EV fast chargers

Merve MOLLAHASANOĞLU^{1*}, Hakkı MOLLAHASANOĞLU², H. İbrahim OKUMUŞ¹

¹Department of Electrical and Electronics Engineering, Karadeniz Technical University, Trabzon, Türkiye

²Department of Electrical and Electronics Engineering, Recep Tayyip Erdoğan University, Rize, Türkiye

Received: 03.05.2023

Accepted/Published Online: 01.10.2023

Final Version: 30.11.2023

Abstract: In this study, the aim is to evaluate three-phase (3ϕ) AC/DC neutral point-clamped (NPC) power factor-corrected (PFC) multilevel converter performance for electric vehicle (EV) fast chargers. Power factor correction for EV fast chargers is very important in terms of efficient power usage and charger compatibility with the grid. Multilevel converters improve charging efficiency, reduce voltage stresses on components, minimize electromagnetic interference, and support high power capabilities. For this reason, multilevel converters with the PFC feature contribute to the reliable and effective operation of the fast-charging infrastructure. Rectifier analysis is tested with extensive simulations using a new modified carrier-based level-shifted pulse-width modulation (PWM) technique. The results obtained are in accordance with international standards. The proposed PWM technique provides low voltage regulation, low total harmonic distortion input current, unit input power factor, and a well-regulated DC bus voltage for the NPC rectifier in fast charging systems, and the system has high efficiency. In addition, the modulation method eliminates the need for an additional PFC circuit. The system demonstrates remarkable success in addressing critical parameters such as capacitor voltage balance. This modified carrier-based PWM is highly successful for NPC rectifiers designed for DC fast chargers, rated for power up to 300 kW. The simulation results of the DC fast charger system demonstrate the validity and flexibility of the proposed carrier-based level-shifted PWM method.

Key words: Battery charger, electric vehicles, carrier-based pulse-width modulation, multilevel converter, power factor correction converter, power quality

1. Introduction

The use of clean and efficient energy sources is very important today. Therefore, the interest in electric vehicles (EVs) is increasing day by day. However, since EV users are concerned about the charging times and ranges of EVs, researchers are focusing on improving the fast-charging infrastructure and batteries of EVs. According to the International Energy Agency (IEA), the number of EV fast chargers increased by 60% in 2019 compared to the previous year. While fast-charging stations increased in number by 43% in 2020 compared to the previous year, the increase in the installation of fast chargers in 2021 was 48%. After 2021, EV fast chargers in Europe increased by over 30% [1]. This has been the motivation for improving the infrastructure of EV fast-charging stations.

The structure of traditional EV fast chargers typically consists of two stages. These are the AC/DC conversion stage, making a power factor correction (PFC), and an isolated DC-DC converter [2]. Figure 1

*Correspondence: merve.aydin@ktu.edu.tr

depicts a typical fast-charging topology. Off-board DC chargers typically require high power, equal to or greater than 50 kW, and are commonly powered by three-phase AC [3]. The filter component comes first in the design, followed by an AC-to-DC conversion stage. Before the plug that connects to the EV, there is an isolated DC-to-DC converter placed within the charger. The charger establishes a direct connection with the EV battery. In order to ensure safe and effective charging, the charger is equipped with a communication link that facilitates communication with the battery management system, allowing for precise control over the charging process and implementation of safety measures [4].

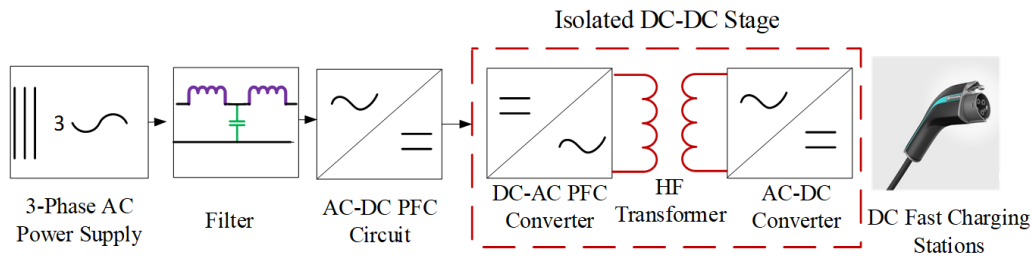


Figure 1. General block diagram of off-board DC fast charger.

AC/DC rectifiers are a key component in off-board EV fast chargers. They are responsible for converting the AC power from the grid into DC power that can be used to charge the EV's battery. In the context of off-board fast chargers, these rectifiers are typically high-power, high-voltage units that can deliver several hundred kilowatts of power to the vehicle's battery in a short amount of time. There are several different types of AC/DC rectifiers that can be used in off-board fast chargers, including diode rectifiers, thyristor rectifiers, and active rectifiers [5]. Each type has its own advantages and disadvantages in terms of efficiency, cost, and complexity. Since diode rectifiers cannot be controlled in EV fast-charging infrastructure, they are not preferred. They are not capable of PFC. On the other hand, thyristor rectifiers cannot correct voltage fluctuations and cannot optimize output voltage control. In addition, thyristors can cause heating problems in high-power applications. This can pose safety risks at fast-charging stations. In fast-charging stations, active rectifier technologies are more flexible and responsive. Therefore, they are preferred to provide output voltage and current requiring precise control. Although active rectifiers have more complex control circuits, they are more efficient, especially for high-power applications due to their PFC capability. Regardless of the types of rectifiers in fast chargers used, their primary function is to convert the AC power from the grid into a form that is compatible with the EV's battery. This is a crucial step in the fast-charging process, as it ensures that the vehicle's battery is charged quickly and efficiently, without damaging the battery or the charger.

The 3ϕ AC/DC rectifier topologies discussed for EV fast chargers are detailed in [6] and [7]. In [6], the rectifier topologies are categorized as unidirectional or bidirectional converters. Unidirectional converters are the T-type Vienna rectifier and buck-type rectifier. Bidirectional converters are two-level voltage source converters (VSCs) and three-level NPC rectifiers. In [7], rectifier topologies are categorized as multilevel and non-multilevel converters. Cascaded H-bridge (CHB) rectifiers, 3ϕ neutral point-clamped (NPC) rectifiers, and 3ϕ flying capacitor multilevel AC/DC converters are multilevel. In [8], it is stated that the primary benefit of utilizing three-level topologies is the reduction of dv/dt voltages on switching devices. To cope with increased power levels, it is necessary to minimize the stress on the components [9]. Thus, it is logical to regard multilevel AC/DC converters as components for EV fast charging. NPC rectifiers can achieve high efficiency and power

density in AC/DC power conversion. These rectifiers operate at higher frequencies and with lower losses. In addition to high efficiency and power density, NPC rectifiers also have other benefits for the fast charging of EVs. For example, they can provide stable output voltage and reduce the impact of harmonic distortion on the grid [10]. Based on the literature reviewed, it is concluded that the NPC rectifier is a crucial component to consider for fast-charging systems of EVs. The NPC rectifier has a multilevel structure, sharing high voltage among components. This reduces the switching losses. The multilevel structure allows multiple voltage levels to be generated and helps to achieve a current waveform with lower harmonics. This improves the charger's power quality. Adjusting the switching states of the rectifier components allows precise control of the output voltage levels. This provides continuous and regulated output voltage. It is important to provide stable power for high power applications like fast-charging stations.

NPC rectifiers are commonly used in high-power applications such as renewable energy systems, motor drives, and industrial power supplies [11]. The control methods for NPC rectifiers typically focus on achieving high power factor, low total harmonic distortion (THD), and fast transient response, as in [12] and [13]. Common control methods used for NPC rectifiers are hysteresis current control [14], pulse-width modulation (PWM) control [15], model predictive control (MPC) [16], and direct power control (DPC) [17]. While controlling the hysteresis current for the NPC rectifier, the target value of the output current is determined. The hysteresis band is in a certain region above and below the target current value. The control system operates in this zone. If the desired current value is outside the hysteresis band, the control system operates. When the control system operates, the switching frequency of the NPC rectifier can be changed and the capacitor voltage can be adjusted [18]. In PWM control for NPC rectifiers, the reference output voltage is compared with the output voltage. The switches are controlled with the PWM signals produced because of the control [19]. For the NPC rectifier, the mathematical model of the system is used in the MPC system. The system behavior is predicted. Based on this estimation, a new system model is realized. Targets and constraints are determined, and optimization is made according to the estimated model [20]. For NPC rectifiers, DPC is used to directly control output power through current and power control loops. DPC adjusts the switching-on and -off times to approach the targeted output power. In this way, the NPC rectifier obtains the desired output power quickly and accurately. However, DPC may require control algorithms and parameter adjustments depending on the specific applications [21]. In this study, PWM control is utilized. This method adjusts the duty cycle of the rectifier's switching signal to regulate the output voltage and current. The proposed PWM control achieves high efficiency, low THD, and low voltage regulation. It also gives the best result in terms of capacitor voltage balance.

The basis of the modulation technique, which is generally applied in multilevel inverters and rectifiers, entails comparison of the reference sine wave and the carrier signal. The switching signal differs with the differentiation of the basic triangular carrier. The modulation technique involving a new carrier signal created by the differentiation of the basic triangle carrier signal is called the modified modulation technique. In the literature, these techniques are called PD-PWM (phase disposition PWM), PD-LSPWM (phase disposition-level shift PWM), modified LS-PWM (level-shift PWM), PS-PWM (phase-shift PWM), POD-PWM (phase opposition disposition PWM), APOD-PWM (asymmetric phase opposition disposition PWM), etc. [22]. There are different modulation methods that can be used to implement PWM control. Space vector PWM (SVPWM) is a more popular form of carrier-based PWM. In the literature, more efficient control is provided by optimizing the space vector [23]. This provides lower THD than traditional carrier-based PWM [24]. In this study, however, the SVPWM method is not considered for the NPC rectifier because the emphasis in this study is to evaluate the performance of modified SPWM types. There are also SHE (selective harmonic elimination) and SHM

(selective harmonic mitigation) PWM methods. The SHE and SHM PWM methods are used to reduce or eliminate harmonics in power electronics systems. SHE is a more flexible technique than SHM, as it allows for the use of multiple switching frequencies and can be applied to a wider range of power electronic systems, as shown in [25] and [26]. Hybrid modulation PWM is commonly used in power electronics applications such as AC/DC and DC-DC converters, as described in [27] and [28]. It has been observed that this method leads to increased efficiency and decreased electromagnetic interference (EMI). In this study, a carrier-based level-shifted PWM modulation technique is optimized to provide more accurate control of switching states in NPC rectifiers considered for implementation in EV fast-charging stations. Different carrier-based PWM techniques available in the literature are also evaluated in this study. When the new modified carrier-based level-shifted PWM technique is compared with the classical triangle carrier PWM, the novel technique appears to be a promising alternative, especially for high-power chargers.

Isolated DC-DC converters are important in EV fast charging because they provide a safe and efficient way to convert the high-voltage DC power from the charging station to the appropriate voltage levels needed by the vehicle's battery [6]. However, the EV battery voltage level can vary depending on the vehicle make and model, which means that the fast charger must be able to provide a range of voltage levels to accommodate different EVs [29]. Isolated DC-DC converters are important in this context because they provide electrical isolation between the fast-charging station and the EV battery, which enhances safety by preventing electrical shocks and reducing the risk of fire or explosion. They also enable efficient power conversion by stepping down the high voltage from the charging station to the lower voltage levels needed by the battery with minimal energy loss, which helps to reduce charging time and improve overall efficiency. Additionally, isolated DC-DC converters can help to address issues related to power quality and stability. For example, they can help mitigate the effects of voltage fluctuations and harmonics, which can occur when multiple charging stations are connected to the same electrical grid [30]. As this study aims to enhance NPC rectifier performance for DC fast-charging stations, the rectifier is evaluated in conjunction with isolated DC-DC converters (DAB) available in the literature, as in [31] and [32].

It is important to keep the output voltage-current ripple of the NPC rectifier and THD of the current drawn from the grid very low. DC voltage ripple should be limited to a maximum of 5% of the nominal voltage for power supplies feeding electronic equipment as per IEEE Standard 1100-2018. In IEEE Standard 519-2014 it is recommended that DC voltage ripple be less than 1% for DC motor drives to prevent adverse effects on motor performance. According to IEEE Standard 519-2014, the recommended THD limit for DC power systems is 3%. Therefore, DC voltage and current ripple and current THD are considered in this study. Furthermore, the power factor is a measure of the efficiency in an electrical system and it is important for it to be equal to 1. While it is desirable to maintain a power factor of 1, the load characteristics, system design, and operating conditions may not always allow this. According to IEEE Standard 1547-2018, industrial systems should have a power factor of at least 0.95, commercial systems should have a power factor of 0.9, and residential systems should have a power factor of 0.8 in power electronics circuits. Modulation is the heart of the converter. Finding the optimum modulation strategy improves power quality. Therefore, power factor and efficiency are also evaluated in this study.

In this study, six different carrier-based level-shifted PWM modulation techniques are evaluated for an NPC rectifier adapted to a fast-charging system. Five of these carrier signals have been discussed in the literature for different converters. However, the proposed modified carrier signal (CS4) gives the most optimal result for the NPC rectifier. Since the system is evaluated for fast charging, it is considered for power values of 50 kW

and above. Only CS4 behaved within acceptable limits for the 300-kW DC fast charger, which has output voltage of 800 V and nominal current of 375 A. This work may inspire other researchers who want to conduct experimental validations.

The main goal of this study is to develop a fast-charging infrastructure. Therefore, the aim is to enhance the observations depicted in Figure 2 for the high-power rectifier under consideration. Figure 2 shows the results examined in this study for all carrier-based level-shifted PWM signals symbolically. Section 2 describes the general structure of the system, the circuit topology, the modulation technique, and the control method. The observations cited in Figure 2 are described in Section 3. Finally, the paper ends with a discussion of the results in Section 4.

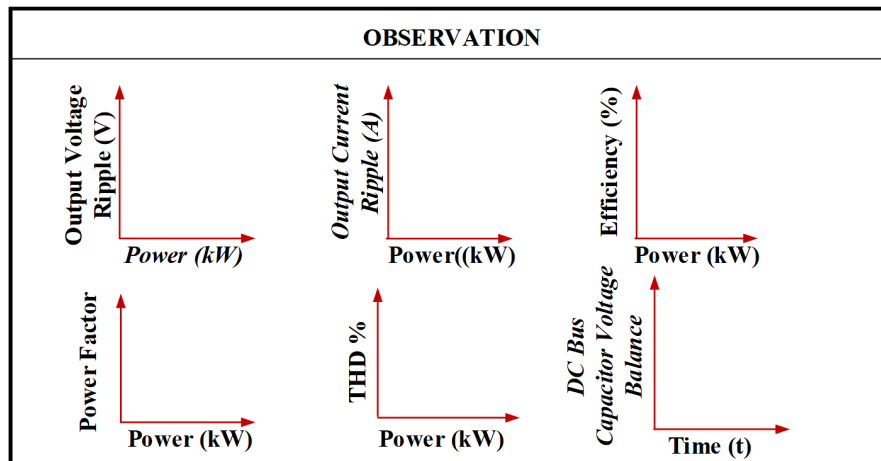


Figure 2. Investigated results of NPC PFC rectifier considered for implementation in EV fast-charging stations.

2. System description

This section explains the operating principle of the NPC rectifier, the modulation technique employed in the study, and the control method utilized.

2.1. Operating principle of the NPC rectifier

The NPC rectifier is a highly effective solution for enhancing power quality at high voltages due to its high-power factor as explained in [12]. When DC chargers are assessed using this rectifier, they exhibit minimal harmonic current, as well as a small load voltage and current ripple factor. The NPC rectifier circuit is shown in Figure 3.

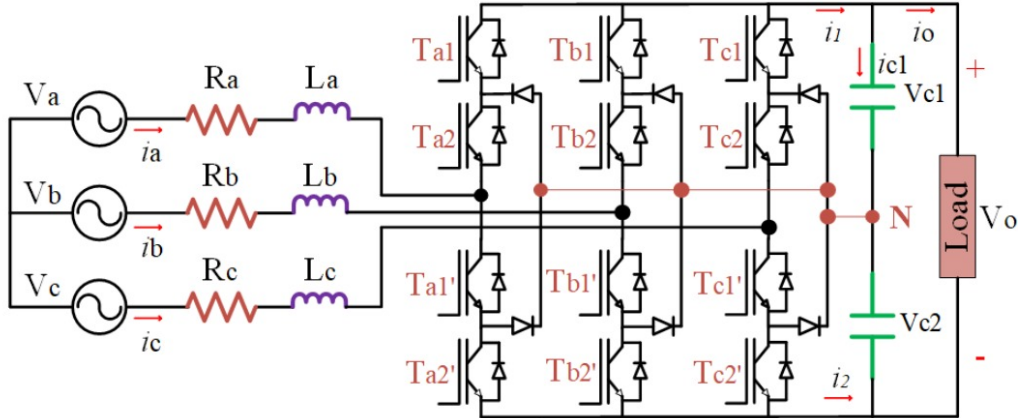


Figure 3. NPC rectifier circuit diagram.

The rectifier input terminal voltages are V_a , V_b , and V_c . Three-phase voltages and line currents are given as in Eqs. (1) and (2), where ω is angular frequency.

$$\begin{aligned} \mathbf{V}_a &= V_m \cos(\omega t) \\ \mathbf{V}_b &= V_m \cos(\omega t - 2\pi/3) \\ \mathbf{V}_c &= V_m \cos(\omega t + 2\pi/3) \end{aligned} \quad (1)$$

$$\begin{aligned} \mathbf{i}_a &= i_m \cos(\omega t) \\ \mathbf{i}_b &= i_m \cos(\omega t - 2\pi/3 + \theta) \\ \mathbf{i}_c &= i_m \cos(\omega t + 2\pi/3 + \theta) \end{aligned} \quad (2)$$

The input voltage at the rectifier AC terminals for the A leg of the converter is given by Eq. (3).

$$\begin{aligned} V_{ao} &= \frac{T_a^2}{2} \Delta V + \frac{T_a^2}{2} V_o \\ V_{bo} &= \frac{T_b^2}{2} \Delta V + \frac{T_b^2}{2} V_o \\ V_{co} &= \frac{T_c^2}{2} \Delta V + \frac{T_c^2}{2} V_o \end{aligned} \quad (3)$$

Here, T_a represents the switching function of the A leg, while T_b and T_c represent the switching functions of legs B and C, respectively. Expression X in Eq. (3) represents any of the A, B, or C phases. T_{x1} is the first switch in phase X. T_{x2} is the second switch in phase X. If T_{x1} is 1, the switch is on; if it is zero, the switch is off.

$\Delta V = V_{C1} - V_{C2}$ and V_o is load voltage. DC bus capacitor voltages V_{C1} and V_{C2} are shown in Figure 3. Load voltage is given by Eq. (4).

$$V_o = V_{C1} + V_{C2} \quad (4)$$

In terms of switching functions, we can write i_1 and i_2 as in Eq. (5).

$$\begin{aligned} i_1 &= \frac{T_a^2 + T_a}{2} i_a + \frac{T_b^2 + T_b}{2} i_b + \frac{T_c^2 + T_c}{2} i_c \\ i_2 &= \frac{T_a^2 - T_a}{2} i_a + \frac{T_b^2 - T_b}{2} i_b + \frac{T_c^2 - T_c}{2} i_c \end{aligned} \quad (5)$$

The currents through the C_1 and C_2 capacitors are given in Eq. (6).

$$\begin{aligned} i_{c1} &= i_1 - i_o \\ i_{c2} &= i_o + i_2 \end{aligned} \quad (6)$$

Here, $i_o = V_o/R_{load}$. Hence, we can write i_{c1} and i_{c2} as in Eq. (7).

$$\begin{aligned} i_{c1} &= \frac{T_a^2 + T_a}{2} i_a + \frac{T_b^2 + T_b}{2} i_b + \frac{T_c^2 + T_c}{2} i_c - \frac{V_o}{R_o} \\ i_{c2} &= \frac{T_a^2 - T_a}{2} i_a + \frac{T_b^2 - T_b}{2} i_b + \frac{T_c^2 - T_c}{2} i_c - \frac{V_o}{R_o} \end{aligned} \quad (7)$$

Capacitor voltages are given by Eq. (8) and they can be obtained in detail as in Eq. (9).

$$\begin{aligned} V_{c1} &= \frac{1}{C_1} \int (i_{c1} - i_o) dt \\ V_{c2} &= \frac{1}{C_2} \int (i_{c2} - i_o) dt \end{aligned} \quad (8)$$

$$\begin{aligned} V_{c1} &= \frac{1}{C_1} \int \left[\left(\frac{T_a^2 + T_a}{2} i_a + \frac{T_b^2 + T_b}{2} i_b + \frac{T_c^2 + T_c}{2} i_c - \frac{V_o}{R_o} \right) \right] dt \\ V_{c2} &= \frac{1}{C_2} \int \left[\left(\frac{T_a^2 - T_a}{2} i_a + \frac{T_b^2 - T_b}{2} i_b + \frac{T_c^2 - T_c}{2} i_c - \frac{V_o}{R_o} \right) \right] dt \end{aligned} \quad (9)$$

In this configuration, the voltage at each switch is only half of the DC bus voltage, as opposed to the full DC bus voltage. As a result, there is less voltage pressure on the switches, which is especially beneficial in high-voltage scenarios. This reduction in voltage stress ultimately leads to lower switching losses. Table 1 shows the switching states for each leg of the rectifier.

Table 1. Switching states and corresponding voltages of the rectifier.

\mathbf{s}	T_{x1}	T_{x2}	$T_{x1'}$	$T_{x2'}$	V_{xn}
1	1	1	0	0	$V_1 = V_0/2$
0	0	1	1	0	0
-1	0	0	1	1	$V_2 = -V_0/2$

Each leg of the rectifier can have four potential switching states, but only three of them are valid to attain three voltage levels at the AC terminals. Figure 4 illustrates the three operating modes for the A leg of the converter, and the same applies to phases B and C.

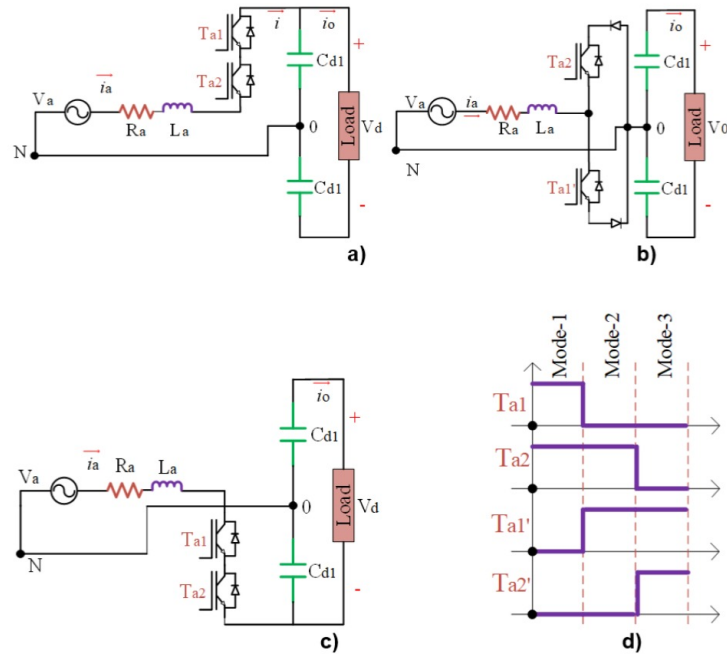


Figure 4. Three operating modes for phase A of NPC PFC rectifier.

2.2. PWM modulation technique

The switching signal of the classical triangular carrier-based SPWM modulation method of the NPC rectifier is shown in Figure 5.

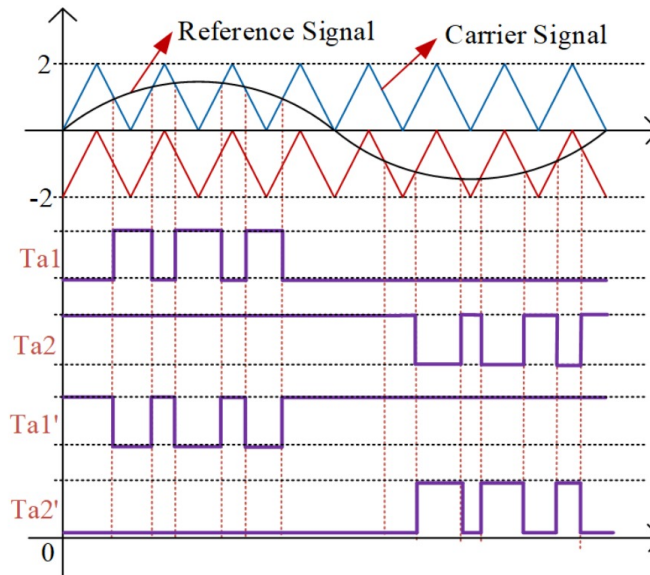


Figure 5. Basic triangular carrier-based level-shifted PWM technique and switching pulses.

The fundamental modulation index value (m_i) is the ratio of the reference sine wave's peak value to the carrier triangle wave's peak value. During the simulation, the frequency of all carriers is 20 kHz and the modulation index is 0.86.

In this study, a sinusoidal waveform is used as the reference modulation signal in generating the switching signal. Various types of waveforms were utilized as the basic carrier signal, which are displayed in Figure 6. Most of the carrier signals employed here are derived from those used in multilevel three-phase rectifiers and inverters. The basis of these carrier signals is the triangle waveform. The carrier signal CS4, as shown in Figure 6d, has not been previously observed in the literature. Carrier signal 1 (CS1) was observed in [33] and is shown in Figure 6a. Similarly, [34] evaluated CS2 (POD-PWM) while [35] evaluated CS3 and CS5, which are shown in Figures 6c and 6e. Furthermore, [36] discussed CS6, as observed in Figure 6f. The modified carrier-based PWM signals (CS3, CS5, and CS6) are also evaluated for a transformerless inverter [37].

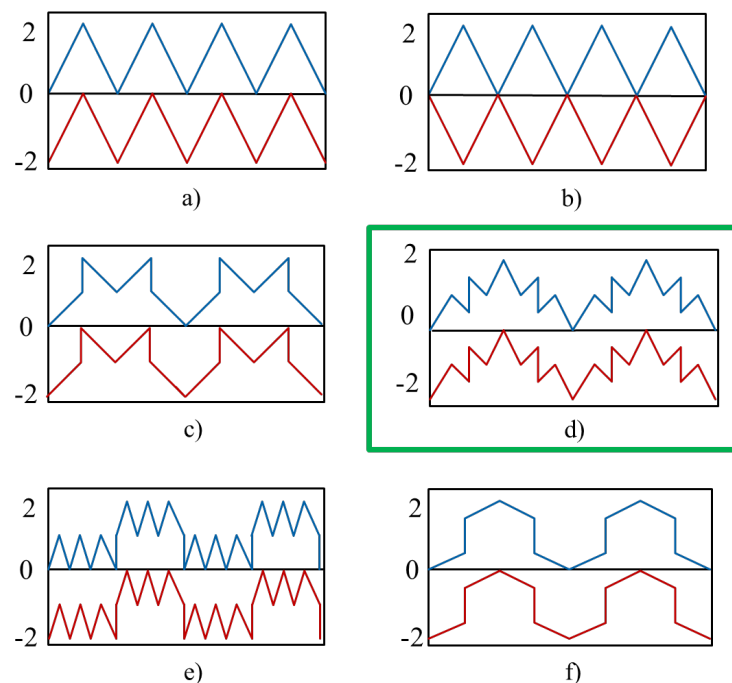


Figure 6. Carrier signal (CS) waveforms evaluated for NPC rectifier.

The traditional basic carrier signal (CS1) and other modified CS types in the literature were compared in this study. Although the switching frequency is the same, the number of fully open and fully closed states of a switch is higher than the others in CS4-based SPWM control in the same period, depending on the type of CS used. This situation affects the parameters shown in Figure 2. CS4 is satisfactory in terms of THD, ripple, capacity balance, throughput, and PF for high-power applications.

Many types of modified carrier-based PWM perform better compared to the traditional carrier signal observed in the literature [38]. This is because the switching frequency is the same but the number of fully open and fully closed states of a switch is high in the same time period, depending on the type of carrier signal used. With the control method performed with the modified carrier-based PWM method, the efficiency of the rectifier increases, the THD value of the output current decreases, and the output voltage and current fluctuation decrease. The PWM signals resulting from the comparison of the proposed carrier signal and the

reference signal are shown in Figure 7. When Figure 7 is examined, it is seen that the number of fully open and fully closed states of the switches is high. This improves the outputs in Figure 2.

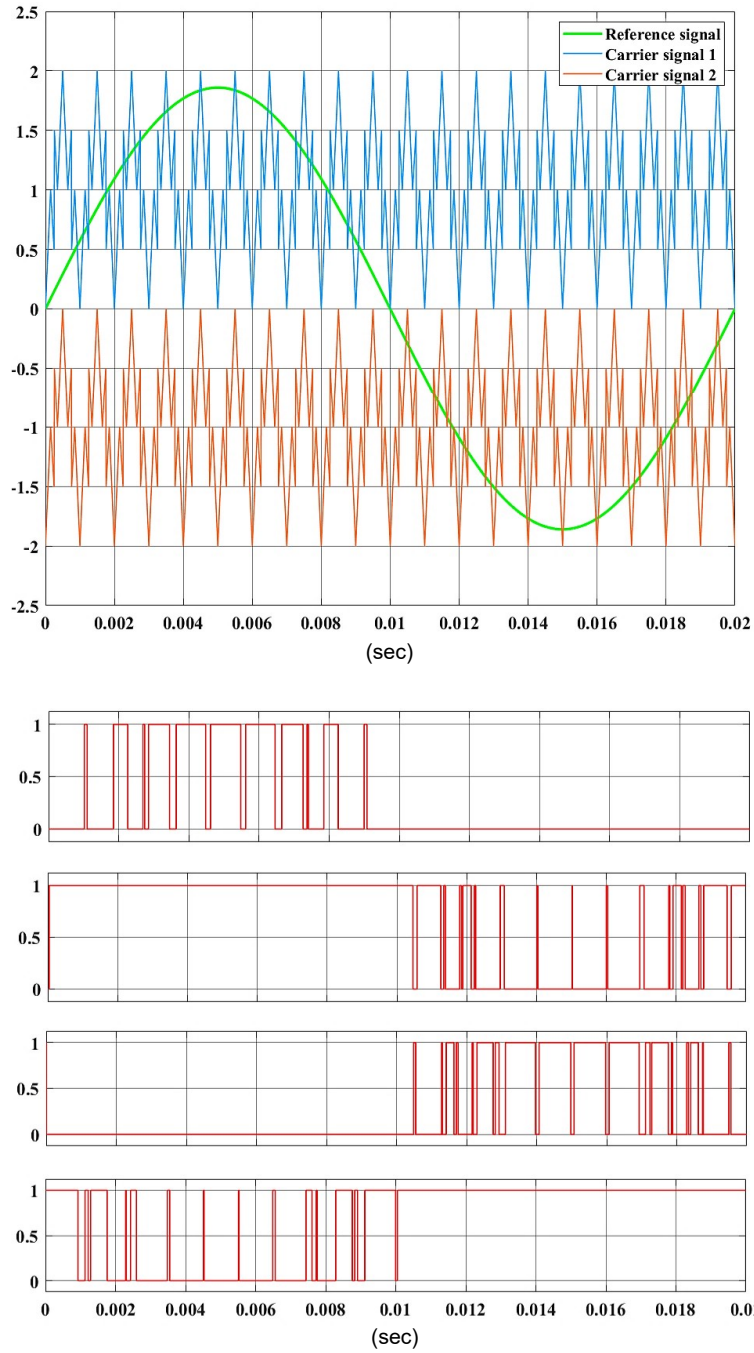


Figure 7. Proposed carrier-based level-shifted PWM technique and switching pulses.

In addition, it is seen that the reference sinus signal is 50 Hz. The reference signal is compared with 20 total CS4 carrier signals in 0.02 s. A carrier signal completes a period in $0.02/20$ s, or 0.001 s.

The proposed carrier signal was created as the sum of the saw tooth signal and the square signal in simulation studies. An example carrier signal of 1 kHz is given in Figure 8. The CS4 carrier signal, which is the sum of the blue square wave and the red saw tooth signal, was evaluated in detail in simulation studies.

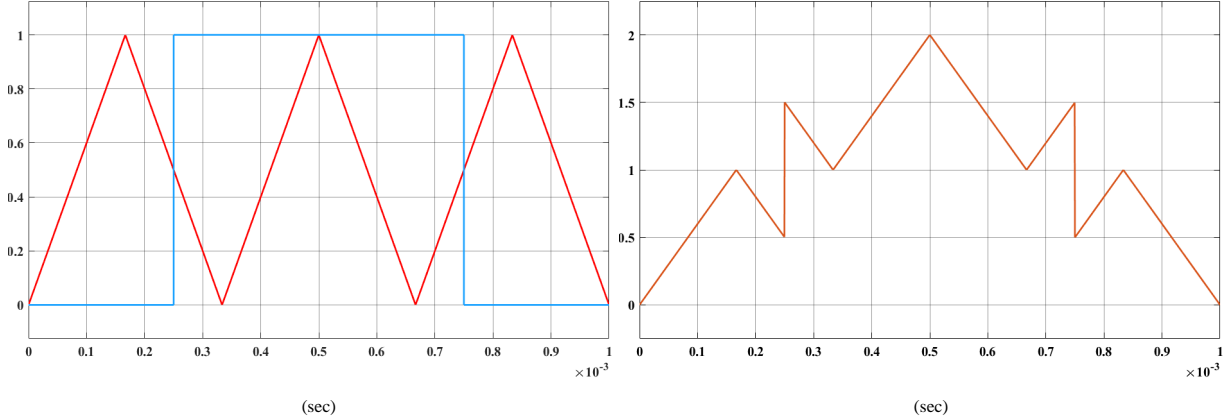


Figure 8. Obtaining the CS4 carrier signal.

2.3. System control

The input terminals of the NPC rectifier are connected to the three-phase source through resistance-inductance R-L. The voltage vector equation can be written as in Eqs. (10) and (11). The source voltage vector V is oriented on the d-axis. The source voltage in the rotating reference (d-q) axis can be expressed by the following equations [39].

$$v_d = L \frac{di_d}{dt} + \omega L i_q + v'_d \quad (10)$$

$$v_q = 0 = L \frac{di_q}{dt} + \omega L i_d + v'_q \quad (11)$$

Here, ω is the 3-phase voltage angular frequency. v_d , v'_d , i_d , v_q , v'_q , and i_q are current-voltage components in the d and q axes. Currents i_d and i_q are controlled by the separated voltages v'_d and v'_q . The control strategy of this rectifier is the same as that used in two-level PWM rectifiers, as in [40]. This is shown in Figure 9.

In this system, the rectifier output voltage is controlled by providing optimum PWM signals. The PI controller is used to control the AC-DC converter output voltage V_{DC} as in Figure 9. The output of this controller, i_{dref} , is used for control, and i_d is the reference for the internal closed loop. The current on the q axis, i_q , is controlled by a similar loop with ($i_{qref}=0$) reference for a high power factor. The V_{dref} and

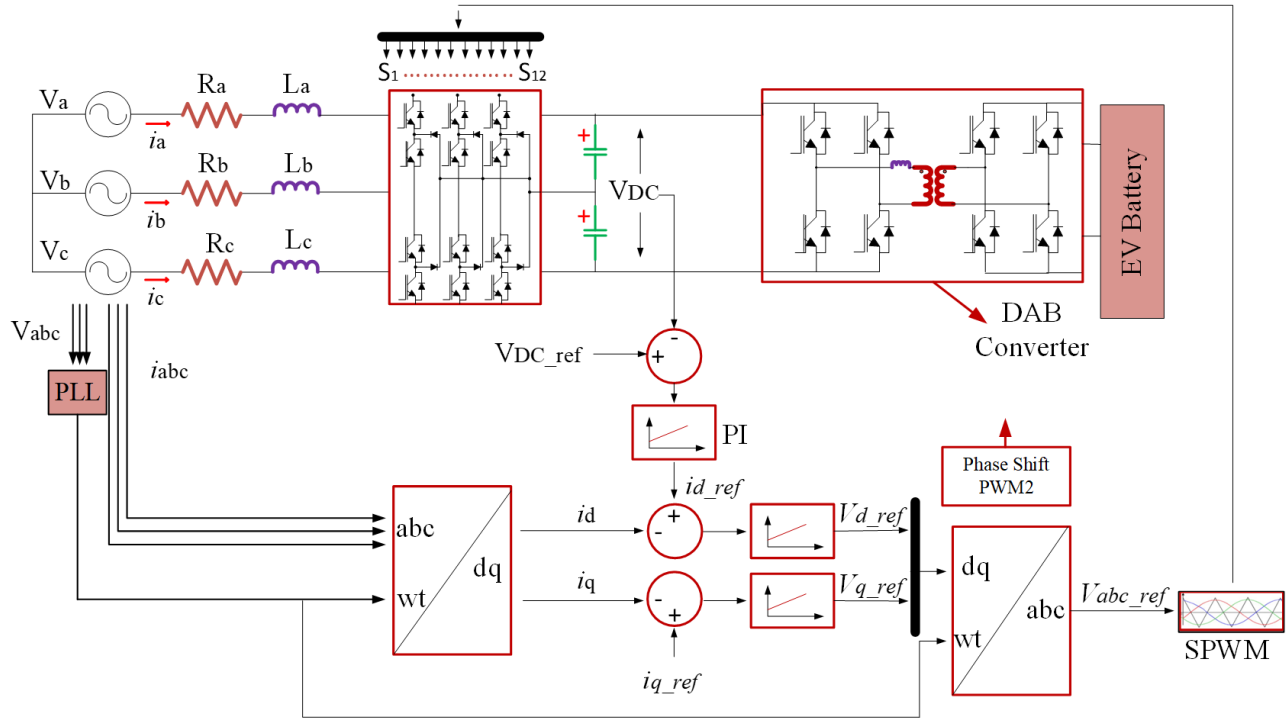


Figure 9. The overall design of the system and control method of the NPC rectifier based on d-q transformation.

V_{qref} reference voltage values on the d and q axes are provided by current controllers, respectively. During the d-q coordinate transformation of the three-phase input voltage, the ωt angle is obtained. This angle is important for generating the switching signals on each leg of the rectifier. An appropriate modulation technique is achieved by controlling the unit sinusoidal signals with a phase difference of 120° taken as a reference for unipolar sinusoidal PWM signals.

In this study, the proposed PWM technique is evaluated in terms of output voltage ripple, the harmonic of the input current, and the power factor for the NPC rectifier. PWM techniques are used because preventing harmonics is important in power electronics applications. PWM techniques are important for energy efficiency. In the literature, THD, power factor, and low voltage regulation are considered when evaluating the performance of AC/DC rectifiers. THD is calculated proportionally to the total root mean square (RMS) value of the harmonic components at the rectifier output. This is shown in Eq. (12). Here, V_n is the RMS magnitude of the n th-order harmonic component [41].

$$THD = \sqrt{\frac{V_2^2 + V_3^2 + V_4^2 + \dots + V_n^2}{V_1^2}} \tag{12}$$

The power factor is based on the phase difference between the input voltage signal and current signal of the AC/DC rectifier circuit. PF is between 0 and 1. It is calculated as in Eq. (13).

$$Power\ Factor\ (PF) = \frac{Active\ Power\ (kW)}{Apparent\ Power\ (kVA)} \tag{13}$$

The voltage regulation of the rectifier is measured by how much the output voltage fluctuates relative to the nominal output voltage. Usually, this ripple changes with load changes or input voltage fluctuations. Low voltage regulation is very important for high-power applications [38]. It is calculated as in Eq. (14).

$$V_{ripple} = \frac{V_{max} - V_{min}}{V_{nominal}} \times 100 \quad (14)$$

3. Performance evaluation and discussion

This section explains how the 3ϕ AC-DC NPC PFC rectifier is valid and flexible for DC fast chargers with the new modulation technique. This study was carried out on the MATLAB/Simulink platform. The elements used in the simulation were SiC MOSFETs, which are frequently preferred for fast chargers. Semiconductor materials and simulation time frame parameters included in the simulation are given in Table 2 in detail. The Simulink interface of the system is shown in Figure 9. When all these parameters are compared with the literature, the system criteria are seen to be suitable for the real world.

Table 2. Switching states and corresponding voltages of the rectifier.

System parameters	Value
Supply side parameters (AC power supply)	$230\sqrt{3}$
Grid frequency	50 Hz
NPC output voltage	800 V
Nominal power	50–300 kW
Switching (carrier) frequency (f_s)	20 kHz
Simulation sampling time (sec)	5e-7
Modulation index (m_i)	0.86
Filter inductance	1 mH
Filter resistance	0.01 Ω
Output capacitances (C_1 and C_2)	5200 μ F
Switches (C3M0060065D Silicon Carbide Power Mosfet) for NPC rectifier	$V_{DSS} = 650$ V $R_{DS(on)} = 60$ m Ω $V_{SD} = 4.8$ V
Power Diodes (APT15D60B)	$V_R = 600$ V $V_F = 1.9$ V
PI (I and V cycle)	$K_p = 0.02, K_i = 10.7$
PI (V_{dc})	$K_p = 0.2, K_i = 90$

In this system, the DAB converter and battery, which are isolated DC-DC converters in EV chargers, are preferred as the nonlinear load for the AC/DC stage. System parameters are determined assuming the AC source voltage is sinusoidal and the DAB converter is lossless. The aim is to observe the behavior of the AC/DC stage for the fast charger, which is a high-power application. This system can also be improved by performing switching losses and thermal analysis with the proposed modulation technique.

The rectifier ripple is calculated as $V_{max} - V_{min}$ in the 0.2nd second. Figure 10 shows the ripples of NPC output voltage and NPC output current for CS4 at 300 kW as an example.

Figures 11a and 11b show voltage and current ripples for different power ratings for all considered CSs. CS1, CS2, CS3, CS4, and CS5 showed less than 1% ripple for both voltage and current from 50 kw to 250 kW.

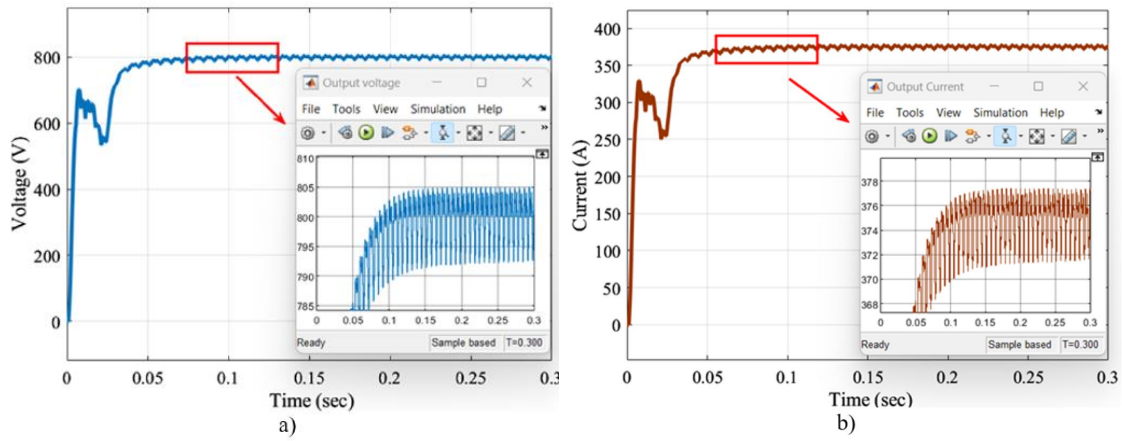


Figure 10. Voltage and current ripples for 300-kW NPC rectifier.

However, only CS4 behaved within acceptable limits from 250 kW to 300 kW.

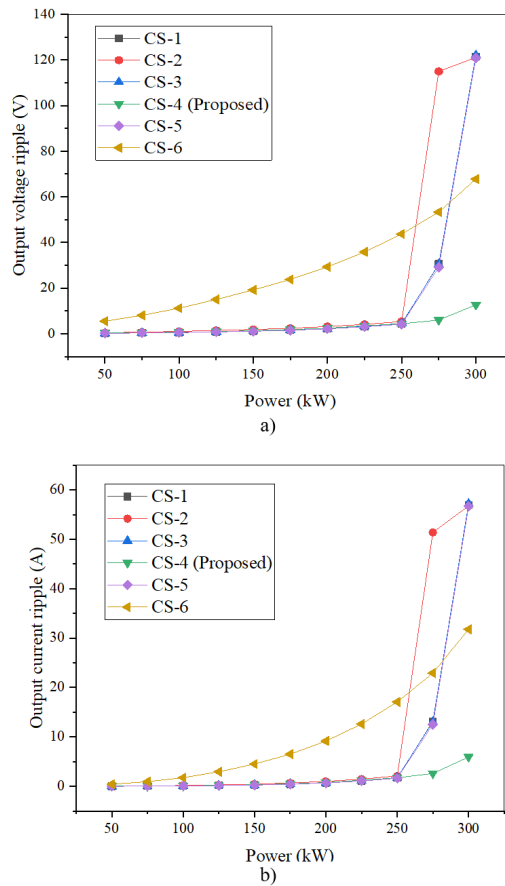


Figure 11. Change of the rectifier output ripples for all CSs from 50 kW to 300 kW: a) voltage ripple, b) current ripple.

Figure 12a shows the terminal inputs of the 300-kW system evaluated with the CS4 PWM technique as an example. Three voltage levels are obtained due to the switching states at the AC terminals of the NPC PFC rectifier. Rectifier input terminal voltage (V_{an}) and grid current (I_{an}) are as in Figure 12b.

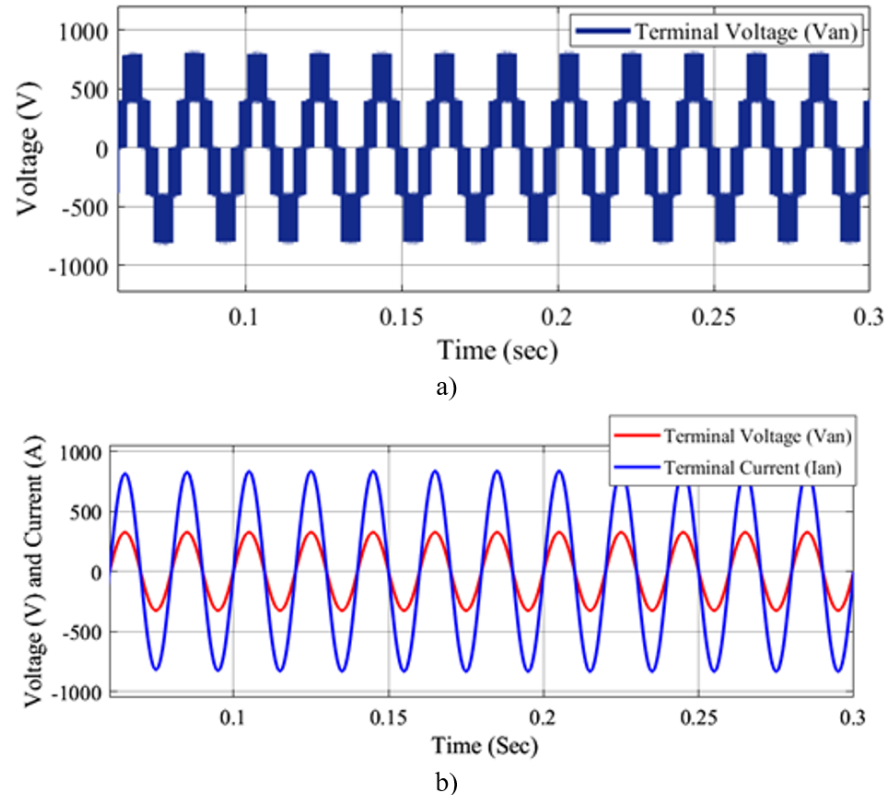


Figure 12. a) Terminal inputs of the 300-kW system evaluated with the CS4 PWM technique and 300-kW NPC rectifier, b) input terminal voltage (V_{an}) and grid current (I_{an}).

Figure 13 shows the change of the power factor value for different power ratings for all CSs. For 300 kW, the power factor is 1 with the CS4-based PWM technique.

The efficiency (η) of the rectifier is calculated as $\eta = P_{out}/P_{in}$ by measuring the input power (P_{in}) and the output power (P_{out}). When we look at Figure 14, the CS4-based PWM modulation technique provides the best efficiency for the 300-kW rectifier.

The CS4-based PWM technique behaves consistently, even at high powers, as shown in Figure 14. Figure 15 shows the FFTs of the current drawn from the AC terminals of the NPC rectifier designed with CS4-based PWM for maximum nominal power. It provides harmonics below 2%.

The CS4-based PWM technique behaves consistently, even at high powers, in terms of THD, as shown in Figure 15. Figure 16 shows the FFTs of the current drawn from the AC terminals of the NPC rectifier designed with CS4-based PWM for maximum nominal power. It provides harmonics below 2%.

Figure 17 shows the capacity balances for all CSs. For 300 kW, the fast-charging system with the NPC rectifier does not balance for CS1, CS2, CS3, CS5, and CS6. However, the CS4-based modulation technique shows capacity balance in a short time. Although it seems to be in balance for CS6, CS6 does not behave consistently in terms of efficiency, THD, power factor, and output ripples.

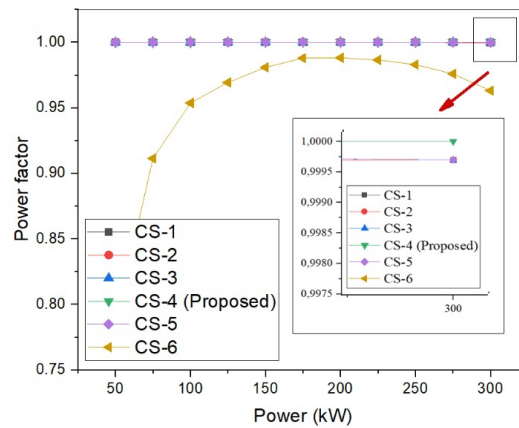


Figure 13. Change of power factor.

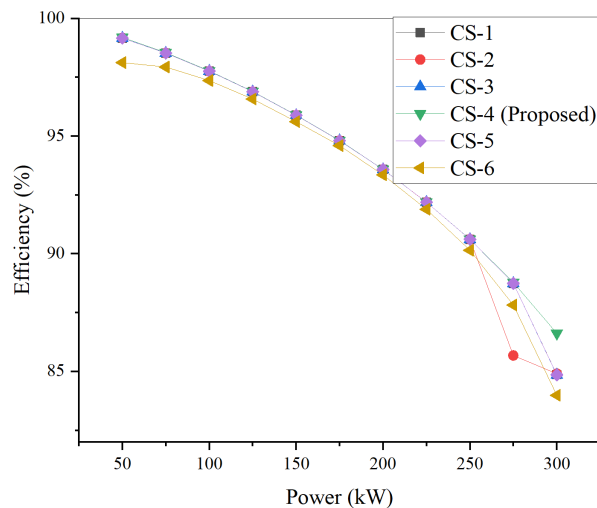


Figure 14. Efficiency of the NPC rectifier for all CSs.

Uncontrollably high currents increase safety risks. With the parameters and switching devices provided in Table 2, the charger system operates under suitable conditions for power of 300 kW. The carriers considered for powers greater than 300 kW do not meet the standards suitable for the charging station. Only CS4 operates within acceptable limits for 300 kW. The voltage stresses for all switches specified in Table 2, used for the NPC rectifier, are within the limits that the switches can withstand.

The proposed CS4-based modulation technique offers successful results, especially for a 300-kW EV charging station. Observations related to the evaluated CS types for the 300-kW charging station are given in Table 3. When the table is examined in detail, the control performed with the CS4-based modulation technique provides more optimum results than the other carrier-based control methods.

When the other AC/DC rectifiers considered for fast charging in the literature are examined, the semiconductor materials number of the NPC rectifier is high. However, the NPC rectifier shows the PFC feature, so it does not require an extra PFC circuit. The high number of elements in the rectifier circuit causes control complexity. However, the absence of an extra PFC circuit is advantageous for high-power applications.

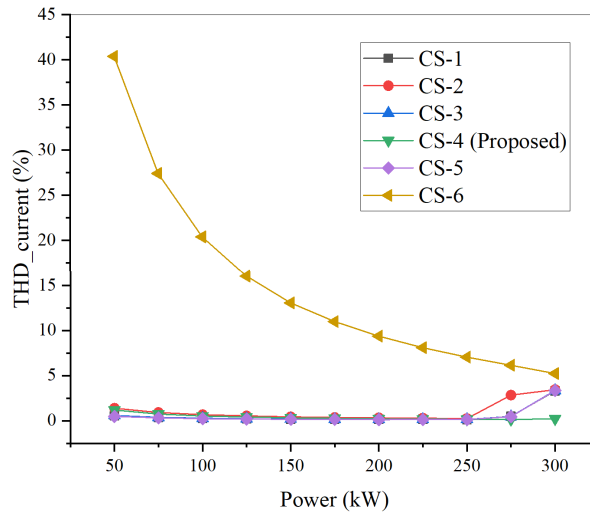


Figure 15. Variation of THD of the NPC rectifier's AC terminal current depending on powers for different CSs.

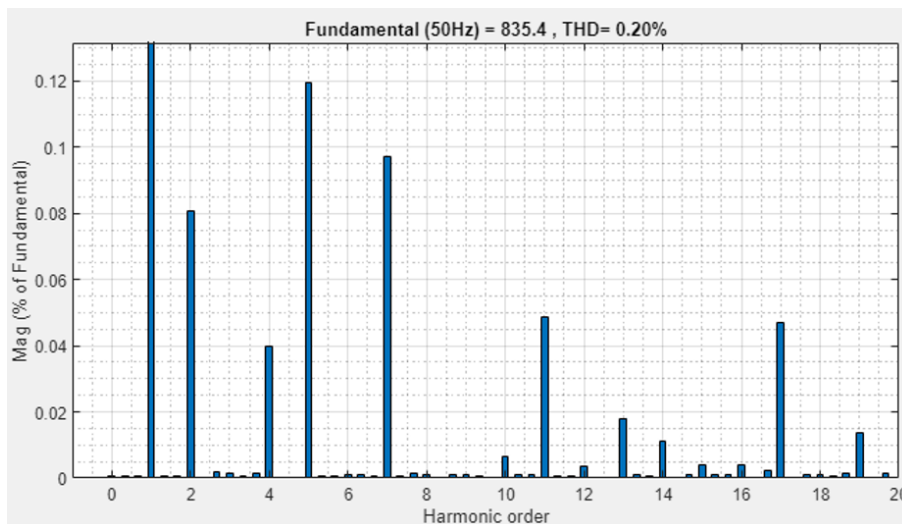


Figure 16. FFTs of NPC rectifier's AC terminal current for 300 kW and CS4.

Table 3. Numerical observation results for 300 kW.

	CS1	CS2	CS3	CS4	CS5	CS6
V_{ripple}	121.45	121.09	122.02	12.67	120.91	67.80
I_{ripple}	56.93	56.77	57.20	5.94	56.68	31.78
THD	3.32	3.45	3.37	0.23	3.36	5.24
Efficiency	84.86	84.89	84.84	86.61	84.85	83.98
PF	0.9997	0.9997	0.9997	1	0.9997	0.963

The proposed modified carrier-based PWM technique yields successful results for EV fast chargers in terms of PFC, efficient power usage, and compatibility of the charger with the grid. The AC/DC NPC rectifier,

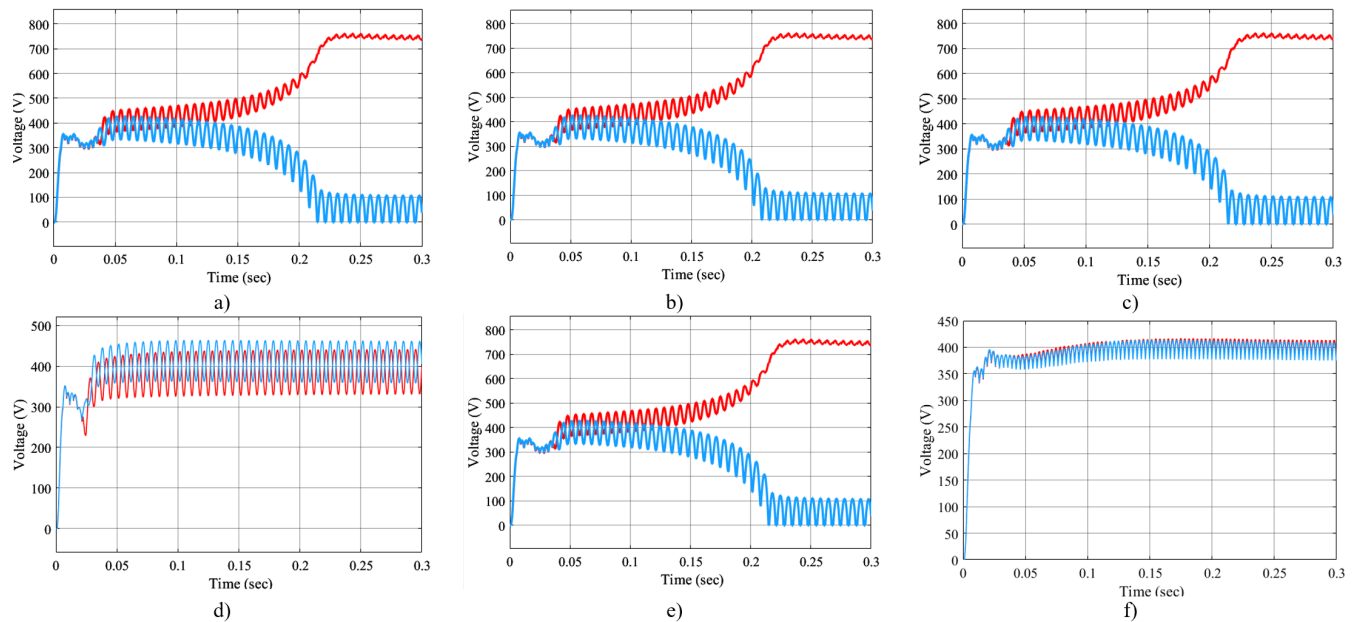


Figure 17. Capacity voltage balance for all carrier-based PWM techniques: a) CS1, b) CS2, c) CS3, d) CS4, e) CS5, and f) CS6.

which is evaluated for charging with the proposed method, supports the fast-charging infrastructure. The proposed new modified carrier signal can be tested with different power electronics circuits. It can also be applied to different AC/DC rectifiers evaluated for fast charging. The system can be further improved from its current state by optimizing the control parameters for the existing system. This is a potential future improvement for high-power applications such as fast chargers.

4. Conclusion

The fast charging of EVs is a high-power application, so it is necessary to draw high current from the grid to charge the EV battery fast. The converters from the grid to the battery operating efficiently and without loss is very important for charging. Furthermore, the power factor being 1 on the grid side and the system complying with the relevant standards are very significant points in the charging of the system. Considering all these factors, it is necessary to find the optimum modulation method. In order to achieve the desired result, research was carried out in the field of carrier-based PWM methods in this study. Carrier signal-based modulation techniques have been used to control the 3-phase AC/DC NPC PFC rectifier in this study. It has been observed that the proposed level-shifted carrier (CS4) derived from the triangular signal is effective for the NPC rectifier. In addition, this study has presented a performance comparison under the same conditions by considering similar techniques in the literature. It has been observed that the NPC rectifier considered for fast charging performs much better than many modified carrier signal types at nominal power of 300 kW when compared to the traditional carrier signal. Although the switching frequency is the same, it is seen that the converter efficiency, systems harmonics, and voltage and current ripple stand out at 300 kW for CS4 depending on the type of CS used. Compared to other carrier-based methods, modulation with CS4 was the technique that offered the most optimum values at high power. The findings of this study may provide inspiration for research

and development of off-board charging solutions for EVs. The AC/DC NPC rectifier evaluated for charging with the proposed method supports the fast-charging infrastructure. The proposed new modified carrier signal can be tested with different power electronics circuits. It can also be applied to different AC/DC rectifiers evaluated for fast charging. The system can be further improved from its current state by optimizing the control parameters for the existing system. This is a potential future improvement for high-power applications such as fast chargers.

Acknowledgment

The authors gratefully thank The Scientific and Technological Research Council of Türkiye (TÜBİTAK), which supported Merve Mollahasanoğlu financially within the scope of the 1002 Short-Term R&D Funding Program (Project Number 123E050).

References

- [1] IEA. Trends in Charging Infrastructure – Global EV Outlook 2022 – Analysis. Paris, France: IEA, 2022. Available at: <https://www.iea.org/reports/global-ev-outlook-2022/trends-in-charging-infrastructure>
- [2] Elserougi A, Abdelsalam I, Massoud A. An isolated-boost-converter-based unidirectional three-phase off-board fast charger for electric vehicles. *IET Electrical Systems in Transportation* 2022; 12: 79-88. <https://doi.org/10.1049/els2.12039>.
- [3] Monteiro V, Afonso J, Sousa T, Afonso JL. The role of off-board EV battery chargers in smart homes and smart grids: operation with renewables and energy storage systems. In: Ahmadian A, Mohammadi-Ivatloo B, Elkamel A (editors). *Electric Vehicles in Energy Systems*. Cham, Switzerland: Springer International Publishing, 2020, pp. 47-72. https://doi.org/10.1007/978-3-030-34448-1_3.
- [4] Saleh SA, Ozkop E, Valdes ME, Yuksel A, Haj-Ahmed M et al. On the factors affecting battery unit contributions to fault currents in grid-connected battery storage systems. *IEEE Transactions on Industry Applications* 2022; 58: 3019-3028. <https://doi.org/10.1109/TIA.2022.3147149>
- [5] Deb N, Singh R, Brooks RR, Bai K. A review of extremely fast charging stations for electric vehicles. *Energies* 2021; 14: 7566. <https://doi.org/10.3390/en14227566>
- [6] Tu H, Feng H, Srdic S, Lukic S. Extreme fast charging of electric vehicles: a technology overview. *IEEE Transactions on Transportation Electrification* 2019; 5: 861-878. <https://doi.org/10.1109/TTE.2019.2958709>
- [7] Safayatullah M, Elrais MT, Ghosh S, Rezaii R, Batarseh I. A comprehensive review of power converter topologies and control methods for electric vehicle fast charging applications. *IEEE Access* 2022; 10: 40753-40793. <https://doi.org/10.1109/ACCESS.2022.3166935>
- [8] Mollahasanoğlu M, Okumuş H. A review of three phase AC-DC power factor correction converters for electric vehicle fast charging. *European Journal of Science and Technology* 2021; 32: 663-669. <https://doi.org/10.31590/ejosat.1041081>
- [9] Saleh SA, Ozkop E, Nahid-Mobarakeh B, Rubaai A, Muttaqi KM et al. Survivability-based protection for three phase permanent magnet synchronous motor drives. In: *IEEE Industry Applications Society Annual Meeting*; Detroit, MI, USA; 2022. pp. 1-8. <https://doi.org/10.1109/IAS54023.2022.9940036>
- [10] Saadaoui A, Ouassaid M, Maaroufi M. Overview of integration of power electronic topologies and advanced control techniques of ultra-fast EV charging stations in standalone microgrids. *Energies* 2023; 16: 1031. <https://doi.org/10.3390/en16031031>
- [11] Zhaksylyk A, Rasool H, Abramushkina E, Chakraborty S, Geury T et al. Review of active front-end rectifiers in EV DC charging applications. *Batteries* 2023; 9: 150. <https://doi.org/10.3390/batteries9030150>

- [12] Sharma D, Bhat AH, Ahmad A, Langer N. Capacitor voltage balancing in neutral-point clamped rectifier using modified modulation index technique. *Computers and Electrical Engineering* 2018; 70: 137-150. <https://doi.org/10.1016/j.compeleceng.2018.02.031>
- [13] Rivera S, Wu B, Kouro S, Yaramasu V, Wang J. Electric vehicle charging station using a neutral point clamped converter with bipolar DC bus. *IEEE Transactions on Industrial Electronics* 2015; 62: 1999-2009. <https://doi.org/10.1109/TIE.2014.2348937>
- [14] Suhara EM, Nandakumar M. Analysis of hysteresis current control techniques for three phase PWM rectifiers. In: 2015 IEEE International Conference on Signal Processing, Informatics, Communication and Energy Systems; Kozhikode, India; 2015. pp. 1-5. <https://doi.org/10.1109/SPICES.2015.7091434>
- [15] Jung JH, Ku HK, Son YD, Kim JM. Open-switch fault diagnosis algorithm and tolerant control method of the three-phase three-level NPC active rectifier. *Energies* 2019; 12: 2495. <https://doi.org/10.3390/en12132495>
- [16] Zhang X, Tan G, Xia T, Wang Q, Wu X. Optimized switching finite control set model predictive control of NPC single-phase three-level rectifiers. *IEEE Transactions on Power Electronics* 2020; 35: 10097-10108. <https://doi.org/10.1109/TPEL.2020.2978185>
- [17] Lahooti Eshkevari A, Arasteh M. Model-predictive direct power control of three-phase three-level NPC PWM rectifier. In: 2017 8th Power Electronics, Drive Systems and Technologies Conference; Mashhad, Iran; 2017. pp. 78-83. <https://doi.org/10.1109/PEDSTC.2017.7910394>
- [18] Okumuş H, Aktaş M. Adaptive hysteresis band control for constant switching frequency in DTC induction machine drives. *Turkish Journal of Electrical Engineering and Computer Sciences* 2010; 18: 59-72. <https://doi.org/10.3906/elk-0812-5>
- [19] Maheshwari AK, Mahar MA, Larik AS, Soomro AH. Design and Analyses of Multi-Carrier Pulse Width Modulation Techniques for Double Level Circuit Based Cascaded H-Bridge Multilevel Inverter. Edmonton, AB, Canada: IIETA, 2021. <https://doi.org/10.18280/ejee.230206>
- [20] Köse H, Aydemir M. A step-down isolated three-phase IGBT boost PFC rectifier using a novel control algorithm with a novel start-up method. *Turkish Journal of Electrical Engineering and Computer Sciences* 2021; 29: 978-993. <https://doi.org/10.3906/elk-2004-176>
- [21] Saleh SA, Ozkop E, Nahid-Mobarakeh B, Rubaai A, Muttaqi KM et al. Survivability-based protection for electric motor drive systems-Part II: Three phase permanent magnet synchronous motor drives. *IEEE Transactions on Industry Applications* 2023; 59: 2760-2771. <https://doi.org/10.1109/TIA.2023.3234518>
- [22] Vijayakumar A, Stonier AA, Peter G, Loganathan AK, Ganji V. Power quality enhancement in asymmetrical cascaded multilevel inverter using modified carrier level shifted pulse width modulation approach. *IET Power Electronics* (in press). <https://doi.org/10.1049/pel2.12429>
- [23] Kefeng L, Fei X, Jilong L, Zhiqin M, Chuanqiang L et al. Space vector pulse width modulation strategy for ANPC-5L inverter based on model predictive control. *IEEE Journal of Emerging and Selected Topics in Power Electronics* (in press). <https://doi.org/10.1109/JESTPE.2023.3257572>
- [24] Kumar MA, Srikanth NV. A comparative study of SPWM and SVPWM controlled HVDC light systems. In: 2013 International Conference Power Energy Control; Dindigul, India; 2013. pp. 591-595. <https://doi.org/10.1109/ICPEC.2013.6527727>
- [25] Pulikanti SR, Konstantinou G, Agelidis VG. Hybrid seven-level cascaded active neutral-point-clamped-based multilevel converter under SHE-PWM. *IEEE Transactions on Industrial Electronics* 2013; 60: 4794-4804. <https://doi.org/10.1109/TIE.2012.2218551>
- [26] Dahidah MSA, Konstantinou G, Agelidis VG. A review of multilevel selective harmonic elimination PWM: formulations, solving algorithms, implementation and applications. *IEEE Transactions on Power Electronics* 2015; 30: 4091-4106. <https://doi.org/10.1109/TPEL.2014.2355226>

- [27] Ahmed A, Biswas SP, Anower MS, Islam MR, Mondal S et al. A hybrid PWM technique to improve the performance of voltage source inverters. *IEEE Access* 2023; 11: 4717-4729. <https://doi.org/10.1109/ACCESS.2023.3235791>
- [28] Montero-Robina P, Albea C, Gómez-Estern F, Gordillo F. Hybrid modeling and control of three-level NPC rectifiers. *Control Engineering Practice* 2023; 130: 105374. <https://doi.org/10.1016/j.conengprac.2022.105374>
- [29] Kang T, Kim C, Suh Y, Park H, Kang B et al. A design and control of bi-directional non-isolated DC-DC converter for rapid electric vehicle charging system. In: 2012 Twenty-Seventh Annual IEEE Applied Power Electronics Conference and Exposition; Orlando, FL, USA; 2012. pp. 14-21. <https://doi.org/10.1109/APEC.2012.6165792>
- [30] Mortezaei A, Abdul-Hak M, Simoes MG. A bidirectional NPC-based level 3 EV charging system with added active filter functionality in smart grid applications. In: 2018 IEEE Transportation Electrification Conference and Expo; Long Beach, CA, USA; 2018. pp. 201-206. <https://doi.org/10.1109/ITEC.2018.8450196>
- [31] Zengin S. A hybrid current modulated DAB DC/DC converter for connecting PV modules to DC grid considering partial shading. *Computers and Electrical Engineering* 2022; 101: 108109. <https://doi.org/10.1016/j.compeleceng.2022.108109>
- [32] Rathore V, Reddy SRP, Rajashekara K. An isolated multilevel DC-DC converter topology with hybrid resonant switching for EV fast charging application. *IEEE Transactions on Industry Applications* 2022; 58: 5546-5557. <https://doi.org/10.1109/TIA.2022.3168504>
- [33] Singh AK, Mandal RK. Switched-capacitor-based five-level inverter with closed-loop control for grid-connected PV application. *Computers and Electrical Engineering* 2023; 108: 108686. <https://doi.org/10.1016/j.compeleceng.2023.108686>
- [34] Chitra S, Valluvan KR. Design and implementation of cascaded H-bridge multilevel inverter using FPGA with multiple carrier phase disposition modulation scheme. *Microprocessors and Microsystems* 2020; 76: 103108. <https://doi.org/10.1016/j.micpro.2020.103108>
- [35] Zhao J, He X, Zhao R. A novel PWM control method for hybrid-clamped multilevel inverters. *IEEE Transactions on Industrial Electronics* 2010; 57: 2365-2373. <https://doi.org/10.1109/TIE.2009.2027915>
- [36] Meraj M, Rahman S, Iqbal A, Al Emadi N. Novel level shifted PWM technique for unequal and equal power sharing in quasi Z-source cascaded multilevel inverter for PV systems. *IEEE Journal of Emerging and Selected Topics in Power Electronics* 2021; 9: 937-948. <https://doi.org/10.1109/JESTPE.2019.2952206>
- [37] Özkop E. Şebeke bağlantılı tek fazlı transformatörsüz evirici için modifiye edilmiş taşıyıcı temelli DGM kontrolü. *EMO Bilimsel Dergi* 2022; 12: 7-14 (in Turkish).
- [38] Ronanki D, Williamson SS. Voltage ripple minimization in modular multilevel converters using modified rotative PWM scheme. In: 2018 AEIT International Annual Conference; Bari, Italy; 2018. pp. 1-6. <https://doi.org/10.23919/AEIT.2018.8577275>
- [39] Saleh SAM, Ozkop E, St-Onge XF, Richard C. Testing the performance of a $dq0$ phaselet transform based digital differential protection for 3ϕ converter transformers. *IEEE Transactions on Industry Applications* 2020; 56: 6258-6271. <https://doi.org/10.1109/TIA.2020.3018702>
- [40] Mallik A, Khaligh A. Comparative study of three-phase buck, boost and buck-boost rectifier topologies for regulated transformer rectifier units. In: 2015 IEEE Transportation Electrification Conference and Expo; Dearborn, MI, USA; 2015. pp. 1-7. <https://doi.org/10.1109/ITEC.2015.7165821>
- [41] Podder S, Biswas MM, Khan MZR. A modified PWM technique to improve total harmonic distortion of multilevel inverter. In: 2016 9th International Conference on Electrical and Computer Engineering; Dhaka, Bangladesh; 2016. pp. 515-518. <https://doi.org/10.1109/ICECE.2016.7853970>